Early bone healing onto implant surface treated by fibronectin/oxysterol for cell adhesion/osteogenic differentiation: *in vivo* experimental study in dogs

Jung-Seok Lee[1,†], Jin-Hyuk Yang[1,†], Ji-Youn Hong[2], Ui-Won Jung[1], Hyeong-Cheol Yang[3], In-Seop Lee[4], Seong-Ho Choi[1,*]

[1]Department of Periodontology, Research Institute for Periodontal Regeneration, Yonsei University College of Dentistry, Seoul, Korea

[2]Department of Periodontology, Kyung Hee University School of Dentistry, Seoul, Korea

[3]Department of Dental Biomaterials Science, Dental Research Institute, Seoul National University School of Dentistry, Seoul, Korea

[4]Atomic-Scale Surface Science Research Center, Yonsei University, Seoul, Korea

pISSN 2093-2278
eISSN 2093-2286

JPIS Journal of Periodontal & Implant Science

Research Article

J Periodontal Implant Sci 2014;44:242-250
http://dx.doi.org/10.5051/jpis.2014.44.5.242

Received: Aug. 30, 2014
Accepted: Sep. 28, 2014

*Correspondence:
Seong-Ho Choi
Department of Periodontology, Yonsei University College of Dentistry, 50 Yonsei-ro, Seodaemun-gu, Seoul 120-752, Korea
E-mail: shchoi726@yuhs.ac
Tel: +82-2-2228-3189
Fax: +82-2-392-0398

†Jung-Seok Lee and Jin-Hyuk Yang contributed equally to this study.

Purpose: This study aimed to evaluate the effects of fibronectin and oxysterol immobilized on machined-surface dental implants for the enhancement of cell attachment and osteogenic differentiation, on peri-implant bone healing in the early healing phase using an experimental model in dogs.

Methods: Five types of dental implants were installed at a healed alveolar ridge in five dogs: a machined-surface implant (MI), apatite-coated MI (AMI), fibronectin-loaded AMI (FAMI), oxysterol-loaded AMI (OAMI), and sand-blasted, large-grit, acid-etched surface implant (SLAI). A randomly selected unilateral ridge was observed for 2 weeks, and the contralateral ridge for a 4-week period. Histologic and histometric analyses were performed for the bone-to-implant contact proportion (BIC) and bone density around the dental implant surface.

Results: Different bone healing patterns were observed according to the type of implant surface 2 weeks after installation; newly formed bone continuously lined the entire surfaces in specimens of the FAMI and SLAI groups, whereas bony trabecula from adjacent bone tissue appeared with minimal new bone lining onto the surface in the MI, AMI, and OAMI groups. Histometric results revealed a significant reduction in the BIC in MI, AMI, and OAMI compared to SLAI, but FAMI demonstrated a comparable BIC with SLAI. Although both the BIC and bone density increased from a 2- to 4-week healing period, bone density showed no significant difference among any of the experimental and control groups.

Conclusions: A fibronectin-coated implant surface designed for cell adhesion could increase contact osteogenesis in the early bone healing phase, but an oxysterol-coated implant surface designed for osteoinductivity could not modify early bone healing around implants in normal bone physiology.

Keywords: Cell adhesion, Dental implants, Fibronectins, Surface properties, Titanium.

INTRODUCTION

Since the dental implant was first introduced, various fixture designs and surface treatments have been developed for enhancement of osseointegration [1,2]. These designs aimed to achieve implant treatment with less time required for the healing period and longer-term clinical stability. Along the above-mentioned lines, machined-surface dental implants were replaced by those with rough surfaces [3]. Notably, sand-blasted, large-grit, acid-etched

dental implants not only provide extensively increased contact area with adjacent alveolar bone tissue [4], but also enhance cell attachment for *de novo* bone formation onto the implant surface [5].

Dental implants are supported by underlying bone tissue via direct bone contact (osseointegration); therefore, increasing the bone-to-implant contact area has been a main research topic in implant dentistry [6,7]. In previous studies, newly formed bone could be observed on the dental implant surface even in fatty marrow areas [8], in which increased bone density was observed around the dental implant compared to the marrow area. These findings can be explained by contact osteogenesis in Davies' hypothesis [5,9]. The author described the mechanism of peri-implant bone healing, in which two types of healing are characterized: differential bone formation from recipient bone (distance) and attached cells onto the implant surface (contact osteogenesis). Therefore, cellular events, including attachment, proliferation, and differentiation on the dental implant surface have been suggested to be the most important factors for peri-implant bone healing and, additionally, Davies [5] proposed that surface topographies also affect contact osteogenesis. Many other studies have proven his hypothesis by demonstrating increased bone-implant contact around rough-surfaced implants [10,11], such as sandblasted, large-grit, and acid-etched surfaces, compared to those with machined surfaces [12,13].

According to the theory of contact osteogenesis, the microtexture of a rough surface could retain fibrin complex on the surface, and enable enhanced attachment and migration of undifferentiated cells, which are the initial steps of bone formation [9,14]. Since the clinical success of these rough surface implants [3,15], various other approaches have been developed for focusing on enhancing cellular events on the modified surfaces, that is, hydrophilic or anodized implant surfaces [16-19]. However, the separate effects of cellular events, such as cell attachment and differentiation, have not yet been elucidated.

The current development of implant surface technology has targeted the generation of a "biomimetic surface" on dental implants [1,20], in which biologic molecules have been applied onto the implant surface to stimulate osteogenesis and mimic each developmental step in the healing process. Extracellular matrix, peptides, and various growth factors are representative biologic molecules. Fibronectin is a major extracellular matrix that mediates attachment of cells to other cells or to other surfaces, such as the basement membrane. Recent studies have introduced a fibronectin-coated dental implant system in the research stage [21,22], and immobilization of fibronectin increased cell attachment [23] and osteoblastic protein expression at the *in vitro* level [24]. Another strategy in creating biomimetic implant surfaces is the use of growth factors [25,26] or their natural substitutes, such as oxysterol [27], for enhancement of osteogenic cell differentiation. Previous studies have demonstrated that oxysterols regulate differentiation of stem cells into osteogenic cells via the hedgehog pathway, and also prevent adipogenic differentiation *in vitro* [28,29]. Another *in vivo* study also found increased bone healing and augmentation in a spinal fusion model in animals [30].

Even though these two types of biomimetic implant surface developments showed increased cell attachment and differentiation *in vitro* [23,27], there was a lack of enhancement of osseointegration by using fibronectin or oxysterol in clinically-mimicking an *in vivo* animal model. Therefore, the present study aimed to evaluate the effects of fibronectin and oxysterol immobilized on machined-surface dental implants for the enhancement of cell attachment and osteogenic differentiation, on peri-implant bone healing in the early healing phase using an experimental model in dogs.

MATERIALS AND METHODS

Animals

Five male mongrel dogs, aged 18–24 months and weighing approximately 30 kg, were used. All of the dogs had intact dentition and a healthy periodontium. Animal selection, management, and preparation, as well as the surgical protocol, followed the routine procedure approved by the Animal Care and Use Committee, Yonsei Medical Center, Seoul, Korea (2011-0072-1).

Implant preparation

Machined-surface implant (MI)

Cylindrical, threaded implants of commercially pure titanium (Ø3.4 mm, 10-mm length) with a machined surface were provided from the Research Institute of Dentium, Seoul, Korea.

Apatite-coated MI (AMI)

The MI was treated by calcium phosphate (CaP) nano-coating at a thickness of 500 nm, using ion beam-assisted deposition, as described previously [22]. For apatite formation on CaP-coated surfaces, samples were immersed into the solution, including Dulbecco's phosphate-buffered saline (DPBS, Gibco-BRL, a division of Life Technology, Grnad Island, NY, USA) and reagent grade $CaCl_2$ (100 mg/L). Apatite-coated samples were then rinsed with distilled water twice and dried at ambient temperature.

Fibronectin-loaded and AMI (FAMI)

FAMI samples were fabricated using the same method as for AMI, except that DPBS solution containing fibronectin was used instead of normal DPBS.

Oxysterol-loaded and AMI (OAMI)

CaP-coated, MIs were immersed in DPBS solution containing oxysterol for 2 days, and washed three times with distilled water and dried. The samples were immersed again in DPBS solution without oxysterol for one more day for additional apatite coating on the oxysterol/apatite coated surface, and then washed and dried.

Sand-blasted, large-grit, acid-etched surface implant (SLAI)

Commercially available dental implants (Implantium, Dentium Co., Seoul, Korea), which were treated by large grit sand-blasting

dx.doi.org/10.5051/jpis.2014.44.5.242

and further etching, were used as a positive control group.

Study design and surgical protocol

Ten experimental groups were allocated according to the type of implant surface (MI, AMI, FAMI, OAMI, and SLAI) and observational period (2 and 4 weeks). Five types of implants were installed in a randomly selected unilateral edentulous ridge, and the same types of implants were installed on the contralateral side at 2 weeks after the first surgery. The order of installation sites was rotated in five animals for even distribution of the experimental site. After allowing differential healing periods (2 and 4 weeks) following implant installation surgery, the animals were sacrificed for histological analysis.

Twelve weeks before implant installation surgery, all premolars and first molars were extracted at both mandibles under general anesthesia and sterile conditions in an operating room using 0.05 mg/kg atropine (subcutaneous injection), 2 mg/kg xylazine (Rompun, Bayer Korea, Seoul, Korea), and 10 mg/kg ketamine hydrochloride (Ketalar, Yuhan Co., Seoul, Korea) intravenously. The dogs were placed on a heating pad, intubated, administered 2% enflurane, and monitored with an electrocardiogram. After disinfecting the surgical sites, 2% lidocaine HCl with epinephrine 1:100,000 (Kwangmyung Pharm, Seoul, Korea) was administered by infiltration at the surgical sites. Implant installation operations were also performed under the same conditions as the tooth extraction procedure. A midcrestal incision was made, and mucoperiosteal flaps were carefully reflected on the buccal and lingual aspects. The edentulous ridge was carefully flattened with a surgical bur under sterile saline irrigation in order to obtain a widened ridge to accommodate a standardized ridge shape. Five prefabricated implants were installed in rotational order from anterior to posterior sites in individual animals with an even distribution of installed sites in each group, and the same order of installed implants was applied at both sides of the edentulous ridge in the same animal. Implant site preparation was performed by sequential drilling, and the flaps were sutured after implant installation using 5-0 resorbable suture materials (Vicryl 5/0, Polyglactin 910, Ethicon, a division of Johnson & Johnson, Somerville, NJ, USA). The sutures were removed after 7–10 days, and a soft diet was provided throughout the study period.

Histologic preparation

The animals were sacrificed with an anesthesia drug overdose, and block sections, including segments of implants, were preserved and fixed in 10% neutral-buffered formalin. The specimens were dehydrated in ethanol, embedded in methacrylate, and sectioned in the mesio-distal plane using a diamond saw (Exakt, Apparatebau, Norderstedt, Germany). From each implant site, a central section was taken to a final thickness of about 30 μm, and the sections were stained with hematoxylin and eosin.

Histologic and histometric analysis

Histologic and histometric analyses were performed using incandescent and polarized light microscopy (Olympus Research System Microscope BX51, Olympus Co., Tokyo, Japan) and a PC-based image analysis system (Image-Pro Plus, Media Cybernetic, Silver Spring, MD, USA). The bone-to-implant contact proportion (BIC) and bone density in the space between two threads were measured along the whole length of the implants. The bone density was defined as the proportion of newly formed bone in the interthread space. At four sites among a total of 50 experimental samples, the implant apex area intruding into the mandibular canal was excluded in the histometric analysis, and this area did not exceed 2 mm in length in any of the four cases (Fig. 1).

Statistical analysis

Statistical analysis was performed using a commercially available software program IBM SPSS Statistics ver. 20.0 (IBM Co., Armonk, NY, USA). The linear mixed model was used to estimate the contributions of two fixed effects (types of surface treatment and observational periods) and a random effect (animal subject) to the histometric results of the bone-to-implant interface (BIC and bone density). Because there was no interaction between the two factors ($P=0.457$ for BIC and $P=0.359$ for bone density), the experimental groups in the same observational period and the same experimental groups with different observational periods were compared separately using repeated measures analysis of variance and a paired *t*-test, respectively. The level of significance was set at 5%.

RESULTS

Clinical observation

After the use of sequential drills and a countersink drill, all implants were installed at the final torque of 30–50 N·m on the day of implant installation. All sites underwent uneventful healing during the whole experimental period, with limited signs of inflammation and cover-screw exposure.

Histologic observation

All specimens, except one implant, showed direct bone contact with the implant surface (osseointegration) along the whole length of the dental implants. One site in the FAMI group showed fibrous encapsulation without any bone contact, and this was excluded in histometric analyses. Four among the 50 installed implants protruded into the mandibular canal, and no bone formation occurred in the protruding area; however, those lengths did not exceed 2 or 3 threads of the dental implant from the apex.

At the observational period of 2 weeks, about half of the dental implant surfaces directly contacted the newly formed bone. Notably, in specimens from the FAMI and SLAI groups, newly formed bone continuously lined the entire surface, while the MIs with and without the other coating methods showed a partial or limited lining of osseointegration (Figs. 1 and 2). Two types of bone trabecula could be observed: One type appeared to sprout from the recipient bone tissue (black asterisks in Fig. 2), and the other type was wo-

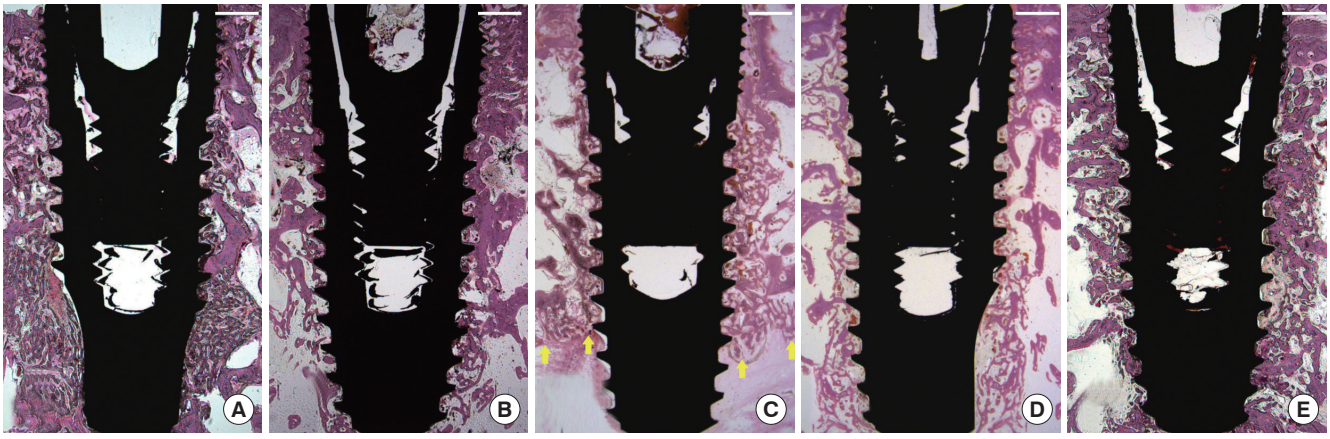

Figure 1. Representative photomicrographs of all experimental and control groups at 2 weeks after implant installation. All specimens showed initial bony healing phases around dental implants, in which woven bone could be found at the prepared or resorbed area of the recipient alveolar bone. An increased number of thin bony trabeculae in newly formed bone was demonstrated in the area adjacent to the implant, including the spaces between threads. There were no significant differences between groups visible at this low magnification. Some implants (4 of a total of 50 experimentally installed implants) protruded into the mandibular canal, due to a lack of height of the residual alveolar ridge (C; arrows indicate superior border of the mandibular canal). These pieces of implant in the canal area were excluded from the histometric analyses. (A) Machined-surface implant (MI), (B) apatite-coated MI (AMI), (C) fibronectin-loaded and AMI, (D) oxysterol-loaded and AMI, and (E) sand-blasted, large-grit, and acid-etched surface implant. The scale bars in all panels were 1 mm.

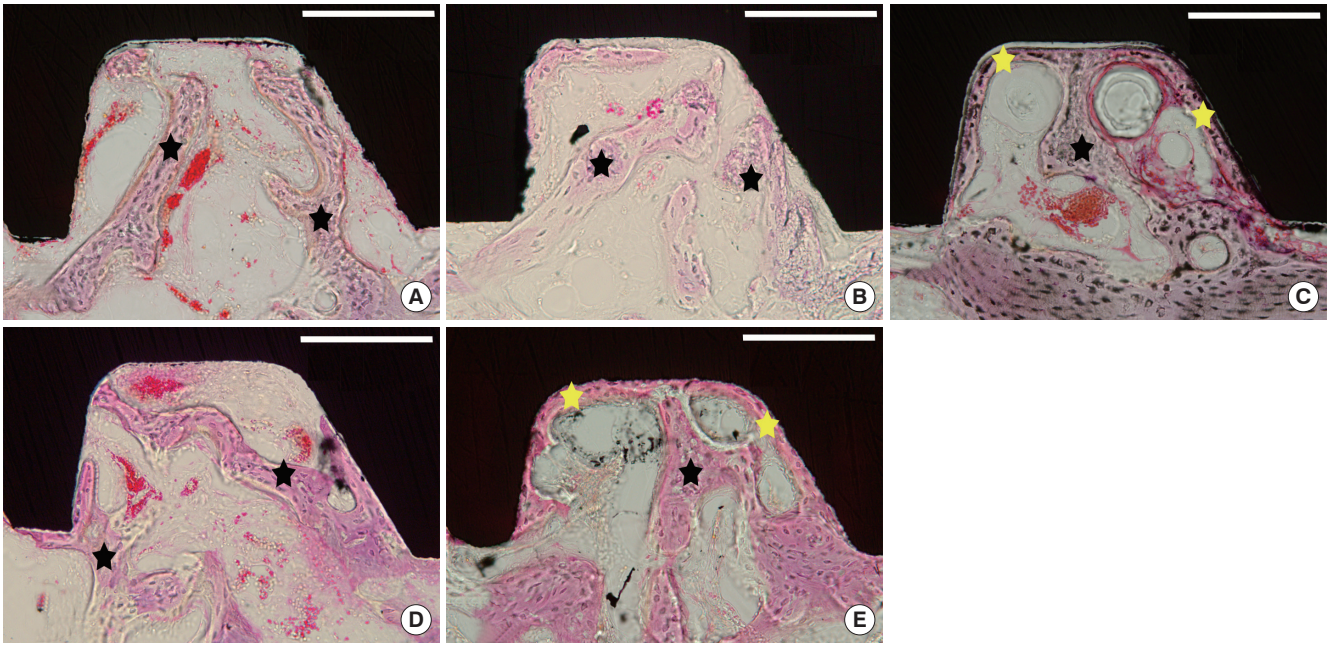

Figure 2. High magnification views of representative experimental and control samples at 2 weeks. All photographs were taken from the middle of the implants, showing the space between the implant threads. In these spaces of machined-surface implant (MI) (A), apatite-coated MI (AMI) (B), and oxysterol-loaded and AMI (D), thin bony trabecula that appeared sprouting from the recipient bone (black asterisks), approached the implant surfaces, whereas fibronectin-loaded and AMI (C) and sand-blasted, large-grit, and acid-etched surface implant (E) showed rims of newly formed bone contacting the implant surface (yellow asterisks) in most of the surface area, indicating contact osteogenesis. The scale bars in all panels represent 100 μm.

ven bone lining newly formed on the implant surface without any relationship with the recipient bone tissue (yellow asterisks in Fig. 2C and E). Most of FAMIs and SLAIs showed the latter type of bone tissue, suggesting contact osteogenesis in the healing processes of osseointegration.

In the specimens from all groups at 4 weeks, newly formed bone tissue increased around the surface and in the space between the implant threads (Figs. 3 and 4). The proportion of newly formed woven bone around the implant was reduced at 4 weeks compared to 2 weeks.

dx.doi.org/10.5051/jpis.2014.44.5.242
JPIS Journal of Periodontal & Implant Science

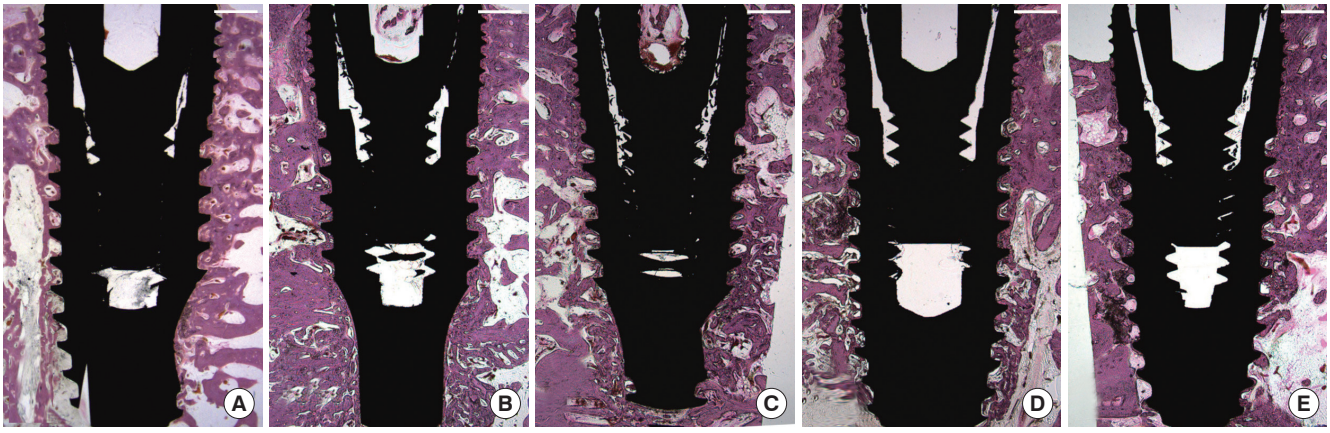

Figure 3. Representative photomicrographs of all experimental and control groups at 4 weeks after implant installation. The woven bone area had decreased in all of the specimens at the 4-week observational period. Most of the spaces between threads were filled with lamellated bone rather than woven bone, and increased, direct contact of bone to dental implants could be found along the whole length of the dental implants. There were still no significant differences in bone healing visible at the bone-to-implant interface in low magnification views. (A) Machined-surface implant (MI), (B) apatite-coated MI (AMI), (C) fibronectin-loaded and AMI, (D) oxysterol-loaded and AMI, and (E) sand-blasted, large-grit, and acid-etched surface implant. The scale bars in all panels represented 1 mm.

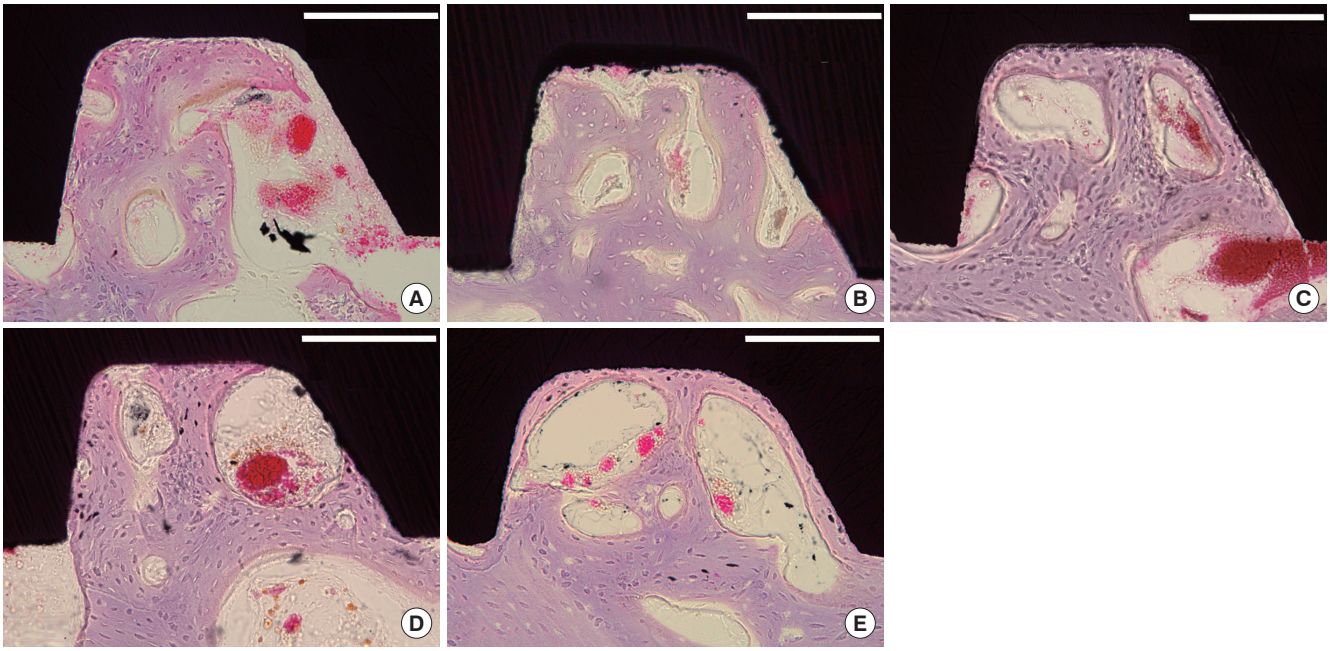

Figure 4. High magnification views of representative experimental and control samples at 4 weeks. All of the spaces between threads were filled with newly formed bone with high density. (A, B, D) Newly formed bone appeared in these spaces, approaching the implant surface from the recipient bone. The newly formed bone was partially in contact with the surface. (C, E) Thickened rims of newly formed bone on the surface could be found at most of the installed implant surface area, and connected with recipient bone tissues or regenerated bone sprouting from the lamellated bone around the dental implants. (A) Machined-surface implant (MI), (B) apatite-coated MI (AMI), (C) fibronectin-loaded and AMI, (D) oxysterol-loaded and AMI, and (E) sand-blasted, large-grit, and acid-etched surface implant. Scale bars in all panels were 100 μm.

Histometric analysis

The results of histometric analyses (mean, standard deviation, and 95% confidence interval for the mean) were presented in Tables 1 and 2 and Fig. 5. Statistical analyses using a linear mixed model revealed that the BICs were significantly different between groups, according to the observational period ($P<0.01$) and type of surface treatment ($P<0.01$). At the 2-week observational period, the BIC averaged 54.08%±9.50%, 59.94%±5.49%, 68.54%±11.42%, 58.65%±8.84%, and 77.14%±7.38% for the MI, AMI, FAMI, OAMI, and SLAI groups, respectively. The SLAI group, as a positive control, showed the highest BIC among all groups, and there were significant differences from the MI ($P<0.01$), AMI

Table 1. Results of histometric analyses in bone-to-implant contact proportion.

Group	2 Weeks		4 Weeks	
	Mean±SD	95% CI	Mean±SD	95% CI
MI	54.08±9.50[a]	42.29–65.88	70.53±7.77[d]	60.88–80.17
AMI	59.94±5.49[b]	52.72–66.36	71.10±11.75[e]	56.51–85.69
FAMI	68.54±11.42	50.37–86.70	73.95±9.74	61.86–86.04
OAMI	58.65±8.84[c]	47.66–69.63	74.94±5.55[f]	68.04–81.83
SLAI	77.14±7.38	67.98–86.30	84.34±4.06	79.30–89.38

SD: standard deviation, CI: confidence interval, MI: machined-surface implant, AMI: apatite-coated MI, FAMI: fibronectin-loaded and AMI, OAMI: oxysterol-loaded and AMI, SLAI: sand-blasted, large-grit, and acid-etched surface implant.
[a]Significantly different between measurements in MI and SLAI groups (P=0.004).
[b]Significantly different between measurements in AMI and SLAI groups (P=0.031).
[c]Significantly different between measurements in OAMI and SLAI groups (P=0.022).
[d,e,f]Significantly different between at 2- and 4-week period measurements in the same group ([d]P=0.019, [e]P=0.042, [f]P=0.015).

Table 2. Results of histometric analyses in bone density.

Group	2 Weeks		4 Weeks	
	Mean±SD	95% CI	Mean±SD	95% CI
MI	29.84±11.80	15.18–44.50	46.92±9.58[a]	35.02–58.82
AMI	33.99±4.57	28.31–39.67	50.82±11.89[b]	36.06–65.58
FAMI	33.78±9.34	18.91–48.65	42.62±3.96	37.71–47.53
OAMI	34.23±8.99	23.07–45.39	51.91±2.86[c]	48.36–55.46
SLAI	42.74±3.42	38.49–46.98	50.18±7.75	40.55–59.80

SD: standard deviation, CI: confidence interval, MI: machined-surface implant, AMI: apatite-coated MI, FAMI: fibronectin-loaded and AMI, OAMI: oxysterol-loaded and AMI, SLAI: sand-blasted, large-grit, and acid-etched surface implant.
[a,b,c]Significantly different between at 2- and 4-week period measurements in the same group ([a]P=0.014, [b]P=0.017, [c]P=0.010).

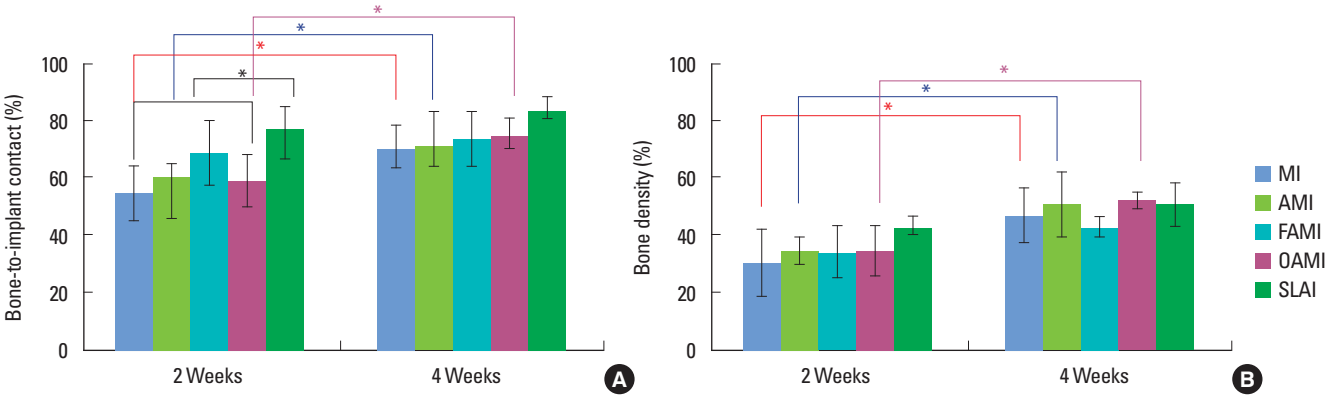

Figure 5. Results of histometric analyses of the proportion of bone-to-implant contact (%) and bone density (%). Asterisks (*) indicate significant differences as shown by statistical analyses. MI: machined-surface implant, AMI: apatite-coated MI, FAMI: fibronectin-loaded and AMI, OAMI: oxysterol-loaded and AMI, SLAI: sand-blasted, large-grit, and acid-etched surface implant.

(P=0.04), and OAMI (P=0.03) groups. Although there was no significant difference in BIC between the FAMI and SLAI groups, the FAMI group had a wider confidence interval for the mean BIC than the SLAI group; a similar maximum level of confidence interval was found in FAMI (86.70%) and SLAI (86.30%), but the corresponding values for the minimum levels of intervals were 50.37% and 67.98%, respectively. The other experimental groups (MI, AMI, and OAMI) showed a significantly increased BIC at 4 weeks compared to the same experimental group at 2 weeks (P=0.03, P=0.04, and P=0.02, respectively). In addition, there were no significant differences in BIC between any of the groups at the 4-week observational period, when the BIC averaged 70.53%±7.77%, 71.10%±11.75%, 73.95%±9.74%, 74.94%±5.55%, and 84.34%±4.06% for the MI, AMI, FAMI, OAMI, and SLAI groups, respectively.

Significantly increased bone density was found from the 2-week to 4-week observational periods in the linear mixed model (P<0.01), but no effects were found according to the type of surface treatment (P=0.134). Bone density at the 2-week observational period averaged 29.84%±11.80%, 33.99%±4.57%, 33.78%±9.34%, 34.23%±8.99%, and 42.74%±3.42% for the MI, AMI, FAMI, OAMI, and SLAI groups, respectively. The corresponding values for bone density at 4 weeks were 46.92%±9.58%, 50.82%±11.89%, 42.62%±3.96%, 51.91%±2.86%, and 50.18%±7.75%, respectively; there were significant differences from 2 weeks to 4 weeks in MI (P=0.02), AMI (P=0.03), and OAMI (P=0.01).

DISCUSSION

This study was based on our two previous studies that demonstrated an increase in cell adhesion on fibronectin and patite-coated titanium surfaces [23] and enhancement of osteoblastic differentiation by oxysterol and apatite-coated titanium surfaces [27]. Since the development of dental implants using titanium, various surface treatments have been studied to make a bioactive titanium surface through the concept of mimicking cellular events in bone formation and remodeling processes [1,20]. The two above-men-

dx.doi.org/10.5051/jpis.2014.44.5.242

tioned types of implant surfaces were also intended to transform the surface from "biotolerant" to "bioactive" titanium: The fibronectin and apatite coating was intended to promote cellular adhesion onto the surface as a first step in the healing process [23], and the oxysterol or apatite coating was intended to promote differentiation of the adhered cells [27]. However, most dental clinicians still prefer rough surface implants without any biomimetic surface modification, even though various types of biomimetic surface implants have been commercially available. A systematic review of the Cochrane Collaboration reported that there was no clinical evidence of superiority in any particular type of dental implant [31].

The present study aimed to determine whether biomimetic implant surfaces that showed greater cell attachment and differentiation at *in vitro* level [23,27] could enhance the histologic parameters of the bone-to-implant interface in experiments *in vivo* mimicking clinical situations. In the present experimental model of normal bone without any defects, two types of bone healing patterns were observed around the dental implant surface: (1) a thin rim of woven bone deposited onto the implant surface (yellow asterisks in Fig. 2); and (2) bony trabecula sprouting from recipient bone tissue and contacting the implant surface (black asterisks in Fig. 2). These correspond to distance osteogenesis and contact osteogenesis in Davies' hypothesis [5], respectively. In a previous study, Davies described contact osteogenesis, in which de novo bone formation occurred on the implant surface; this pattern of healing was also demonstrated in the present results [5,9]. At the 2-week observational period, mineralized tissue could be seen on the implant surface contacting connective tissue fibers. Furthermore, the thickness and degrees of mineralization were varied, which indicated the bone formation process originated from the implant surface rather than the recipient bone tissue.

The sites receiving FAMI showed histologic evidence of contact osteogenesis along a larger area of the implant surface compared to the other experimental groups at 2 weeks of healing. The first step in contact osteogenesis would be cell adhesion onto the implant surface, followed by further cellular events, including proliferation and differentiation [14]. Fibronectin binds to cell adhesion molecules (integrin) on the cell surface, and increases/stabilizes cell-cell/cell-stratum adhesion [32,33]; therefore, these *in vivo* results might be caused by the function of fibronectin, like *in vitro* results. This healing pattern could also be demonstrated in sites receiving SLAI as a positive control group. Numerous previous studies have already found increased bone-to-implant contact in SLA-surfaced implants compared to MIs, which resulted from increased surface energy by microroughness of the surface [13,34,35]. In the histometric results, the SLAI group showed a higher BIC compared to the other three experimental groups (MI, AMI, and OAMI), and there was no significant difference between the FAMI and SLAI groups. However, the FAMI group also did not show any differences from the other groups, unlike the SLAI group. While the SLAI group showed a narrow range of histometric results, sites receiving FAMI showed a relatively wide range of results with regard to the BIC proportion; 95% confidence intervals for the mean were 67.98–86.30 in the SLAI group and 50.37–86.70 in the FAMI group. Rough surface implants can provide increased contact surface and mechanical interlocking with the recipient bone tissue [11,36], and these might increase the stability of SLAI during the early healing period. Increasing the stability of implants could also stabilize the *in vivo* healing process, which can be influenced by not only cellular events, but also the various environments of the recipient site (bone quality, biologic responses by cytokines, and immune responses). For this reason, FAMI might show a less uniform increase in the BIC compared to the SLAI, despite enhancement of cell adhesion.

Oxysterol is an oxidized derivative of cholesterol, and its novel characteristic of regulating differentiation into osteogenic cells has been the subject of increasing research attention. In previous studies, oxysterol induced *in vivo* osteogenesis like bone morphogenetic protein-2 (BMP-2), or synergistically increased the osteoinductive effects of BMP-2 [30,37,38]. Since complications of BMP-2 application have emerged in research and clinical fields [39,40], oxysterol has received attention as a substitute or regulating factor for BMP-2. Our previous study also showed an increase in alkaline phosphatase with oxysterol surface coating, and simultaneous apatite and oxysterol coating could synergistically enhance *in vitro* osteogenesis [27]. In the present study, the authors hypothesized that osteoinduction by oxysterol could enhance bone formation by osteoblasts adhered to the implant surface, and increase the BIC and bone density in the early healing phase. However, oxysterol coating on the implant surface failed to enhance the BIC and bone density in the space between threads, and these findings are in agreement with a previous study [26] that demonstrated that implant surface coating with recombinant human BMP-2 did not increase the BIC or bone density in a nondefect, normal bone area, despite successful vertical augmentation in the supra-alveolar defect area without any graft materials [25,26]. Osteoinductive molecules might not accelerate or enhance bone healing at the bone-to-implant interface in normal bone, even though they can increase bone formation in the area with unfavorable defects. However, to confirm these hypotheses, further studies should be performed in various defect models.

This study aimed to determine the effects of enhancement of cell adhesion onto the implant surface and osteogenic differentiation by surface coating techniques on bone healing processes, especially at the bone-to-implant interface, in the early healing phase. Two types of implants focusing on cell adhesion increased the BIC at 2 weeks after implant installation: sand-blasted/acid-etched and fibronectin-coated surface implants. However, surface coating with osteoinductive molecules did not modify the BIC or bone density around any of the implant surfaces. Cell adhesion onto the implant surface may enhance contact osteogenesis around the implant in the early healing phase, when the implant is installed in normal bone without any defect.

CONFLICT OF INTEREST

No potential conflict of interest relevant to this article was reported.

ACKNOWLEDGEMENTS

This research was supported by the Basic Science Research Program through the National Research Foundation of Korea (NRF) funded by the Ministry of Education (NRF-2013R1A1A2060464).

ORCID

Jung-Seok Lee *http://orcid.org/0000-0003-1276-5978*
Jin-Hyuk Yang *http://orcid.org/0000-0002-8238-1374*
Ji-Youn Hong *http://orcid.org/0000-0003-1040-7077*
Ui-Won Jung *http://orcid.org/0000-0001-6371-4172*
Hyeong-Cheol Yang *http://orcid.org/0000-0001-9420-7894*
In-Seop Lee *http://orcid.org/0000-0002-0407-0431*
Seong-Ho Choi *http://orcid.org/0000-0001-6704-6124*

REFERENCES

1. Choi AH, Ben-Nissan B, Matinlinna JP, Conway RC. Current perspectives: calcium phosphate nanocoatings and nanocomposite coatings in dentistry. J Dent Res 2013;92:853-9.
2. Sykaras N, Iacopino AM, Marker VA, Triplett RG, Woody RD. Implant materials, designs, and surface topographies: their effect on osseointegration: a literature review. Int J Oral Maxillofac Implants 2000;15:675-90.
3. Scacchi M, Merz BR, Schar AR. The development of the ITI DENTAL IMPLANT SYSTEM. Part 2: 1998-2000: Steps into the next millennium. Clin Oral Implants Res 2000;11 Suppl 1:22-32.
4. Cochran DL, Schenk RK, Lussi A, Higginbottom FL, Buser D. Bone response to unloaded and loaded titanium implants with a sandblasted and acid-etched surface: a histometric study in the canine mandible. J Biomed Mater Res 1998;40:1-11.
5. Davies JE. Mechanisms of endosseous integration. Int J Prosthodont 1998;11:391-401.
6. Weber HP, Fiorellini JP. The biology and morphology of the implant-tissue interface. Alpha Omegan 1992;85:61-4.
7. Albrektsson T, Branemark PI, Hansson HA, Lindstrom J. Osseointegrated titanium implants. Requirements for ensuring a long-lasting, direct bone-to-implant anchorage in man. Acta Orthop Scand 1981;52:155-70.
8. Rahal MD, Branemark PI, Osmond DG. Response of bone marrow to titanium implants: osseointegration and the establishment of a bone marrow-titanium interface in mice. Int J Oral Maxillofac Implants 1993;8:573-9.
9. Davies JE. Understanding peri-implant endosseous healing. J Dent Educ 2003;67:932-49.
10. Ericsson I, Johansson CB, Bystedt H, Norton MR. A histomorphometric evaluation of bone-to-implant contact on machine-prepared and roughened titanium dental implants: a pilot study in the dog. Clin Oral Implants Res 1994;5:202-6.
11. Cooper LF. A role for surface topography in creating and maintaining bone at titanium endosseous implants. J Prosthet Dent 2000;84:522-34.
12. Buser D, Nydegger T, Oxland T, Cochran DL, Schenk RK, Hirt HP, et al. Interface shear strength of titanium implants with a sandblasted and acid-etched surface: a biomechanical study in the maxilla of miniature pigs. J Biomed Mater Res 1999;45:75-83.
13. Buser D, Schenk RK, Steinemann S, Fiorellini JP, Fox CH, Stich H. Influence of surface characteristics on bone integration of titanium implants: a histomorphometric study in miniature pigs. J Biomed Mater Res 1991;25:889-902.
14. Park JY, Gemmell CH, Davies JE. Platelet interactions with titanium: modulation of platelet activity by surface topography. Biomaterials 2001;22:2671-82.
15. Cochran DL, Buser D, ten Bruggenkate CM, Weingart D, Taylor TM, Bernard JP, et al. The use of reduced healing times on ITI implants with a sandblasted and acid-etched (SLA) surface: early results from clinical trials on ITI SLA implants. Clin Oral Implants Res 2002;13:144-53.
16. Lai HC, Zhuang LF, Liu X, Wieland M, Zhang ZY, Zhang ZY. The influence of surface energy on early adherent events of osteoblast on titanium substrates. J Biomed Mater Res A 2010;93:289-96.
17. Wall I, Donos N, Carlqvist K, Jones F, Brett P. Modified titanium surfaces promote accelerated osteogenic differentiation of mesenchymal stromal cells in vitro. Bone 2009;45:17-26.
18. Qu Z, Rausch-Fan X, Wieland M, Matejka M, Schedle A. The initial attachment and subsequent behavior regulation of osteoblasts by dental implant surface modification. J Biomed Mater Res A 2007;82:658-68.
19. Li Y, Lee IS, Cui FZ, Choi SH. The biocompatibility of nanostructured calcium phosphate coated on micro-arc oxidized titanium. Biomaterials 2008;29:2025-32.
20. Le Guehennec L, Soueidan A, Layrolle P, Amouriq Y. Surface treatments of titanium dental implants for rapid osseointegration. Dent Mater 2007;23:844-54.
21. Kim S, Myung WC, Lee JS, Cha JK, Jung UW, Yang HC, et al. The effect of fibronectin-coated implant on canine osseointegration. J Periodontal Implant Sci 2011;41:242-7.
22. Hilbig H, Kirsten M, Rupietta R, Graf HL, Thalhammer S, Strasser S, et al. Implant surface coatings with bone sialoprotein, collagen, and fibronectin and their effects on cells derived from human maxillar bone. Eur J Med Res 2007;12:6-12.
23. Chen C, Lee IS, Zhang SM, Yang HC. Biomimetic apatite formation on calcium phosphate-coated titanium in Dulbecco's phosphate-buffered saline solution containing CaCl(2) with and without fibronectin. Acta Biomater 2010;6:2274-81.
24. Gorbahn M, Klein MO, Lehnert M, Ziebart T, Brullmann D, Koper I, et al. Promotion of osteogenic cell response using quasicovalent immobilized fibronectin on titanium surfaces: introduction of a

novel biomimetic layer system. J Oral Maxillofac Surg 2012;70:1827-34.
25. Leknes KN, Yang J, Qahash M, Polimeni G, Susin C, Wikesjo UM. Alveolar ridge augmentation using implants coated with recombinant human bone morphogenetic protein-2: radiographic observations. Clin Oral Implants Res 2008;19:1027-33.
26. Wikesjo UM, Qahash M, Polimeni G, Susin C, Shanaman RH, Rohrer MD, et al. Alveolar ridge augmentation using implants coated with recombinant human bone morphogenetic protein-2: histologic observations. J Clin Periodontol 2008;35:1001-10.
27. Son KM, Park HC, Kim NR, Lee IS, Yang HC. Enhancement of the ALP activity of C3H10T1/2 cells by the combination of an oxysterol and apatite. Biomed Mater 2010;5:044107.
28. Stappenbeck F, Xiao W, Epperson M, Riley M, Priest A, Huang D, et al. Novel oxysterols activate the Hedgehog pathway and induce osteogenesis. Bioorg Med Chem Lett 2012;22:5893-7.
29. Aghaloo TL, Amantea CM, Cowan CM, Richardson JA, Wu BM, Parhami F, et al. Oxysterols enhance osteoblast differentiation in vitro and bone healing in vivo. J Orthop Res 2007;25:1488-97.
30. Johnson JS, Meliton V, Kim WK, Lee KB, Wang JC, Nguyen K, et al. Novel oxysterols have pro-osteogenic and anti-adipogenic effects in vitro and induce spinal fusion in vivo. J Cell Biochem 2011;112:1673-84.
31. Esposito M, Murray-Curtis L, Grusovin MG, Coulthard P, Worthington HV. Interventions for replacing missing teeth: different types of dental implants. Cochrane Database Syst Rev 2007;(4):CD003815.
32. Hynes RO. Integrins: versatility, modulation, and signaling in cell adhesion. Cell 1992;69:11-25.
33. Parsons JT, Horwitz AR, Schwartz MA. Cell adhesion: integrating cytoskeletal dynamics and cellular tension. Nat Rev Mol Cell Biol 2010;11:633-43.
34. Abrahamsson I, Berglundh T, Linder E, Lang NP, Lindhe J. Early bone formation adjacent to rough and turned endosseous implant surfaces: an experimental study in the dog. Clin Oral Implants Res 2004;15:381-92.
35. Piattelli A, Manzon L, Scarano A, Paolantonio M, Piattelli M. Histologic and histomorphometric analysis of the bone response to machined and sandblasted titanium implants: an experimental study in rabbits. Int J Oral Maxillofac Implants 1998;13:805-10.
36. Li D, Ferguson SJ, Beutler T, Cochran DL, Sittig C, Hirt HP, et al. Biomechanical comparison of the sandblasted and acid-etched and the machined and acid-etched titanium surface for dental implants. J Biomed Mater Res 2002;60:325-32.
37. Amantea CM, Kim WK, Meliton V, Tetradis S, Parhami F. Oxysterol-induced osteogenic differentiation of marrow stromal cells is regulated by Dkk-1 inhibitable and PI3-kinase mediated signaling. J Cell Biochem 2008;105:424-36.
38. Kha HT, Basseri B, Shouhed D, Richardson J, Tetradis S, Hahn TJ, et al. Oxysterols regulate differentiation of mesenchymal stem cells: pro-bone and anti-fat. J Bone Miner Res 2004;19:830-40.
39. Choi Y, Lee JS, Kim YJ, Kim MS, Choi SH, Cho KS, et al. Recombinant human bone morphogenetic protein-2 stimulates the osteogenic potential of the Schneiderian membrane: a histometric analysis in rabbits. Tissue Eng Part A 2013;19:1994-2004.
40. Zara JN, Siu RK, Zhang X, Shen J, Ngo R, Lee M, et al. High doses of bone morphogenetic protein 2 induce structurally abnormal bone and inflammation in vivo. Tissue Eng Part A 2011;17:1389-99.